

## Numerical Analysis of the Interaction Between a Fixed FPSO Benchmark Model and Focused Waves

*Qi Li, Yuan Zhuang, Decheng Wan\*, Gang Chen*

Collaborative Innovation Center for Advanced Ship and Deep-Sea Exploration, State Key Laboratory of Ocean Engineering, School of Naval Architecture, Ocean and Civil Engineering, Shanghai Jiao Tong University, Shanghai, China

\*Corresponding author

### ABSTRACT

To study the requested blind test, our in-house two-phase flow solver naoe-FOAM-SJTU is applied to simulate the wave-structure interaction problem between focused waves and the FPSO benchmark model. According to the experimental requirements, a series of focused waves with different wave steepness ( $kA=0.13, 0.18$  and  $0.21$ ) are generated using underlying JONSWAP Spectrum. The validation work shows a good correlation when comparing the numerical wave elevation results of focused waves with the corresponding experimental results. On the basis of effective wave environments, the pressures on the FPSO bow are calculated. The diffraction effect and the wave run-up phenomenon around the FPSO hull in different wave steepness are discussed to explain the blind calculation results.

**KEY WORDS:** Focused wave; FPSO; blind test; naoe-FOAM-SJTU solver; wave steepness.

### INTRODUCTION

Dangerous extreme waves like focused waves are more possibly impact on the marine architectures which are dispatched to a particular place for a long-term production operation. Due to the potential method cannot solve the extreme sea states with strong non-linear phenomenon, the advantages of CFD method arouse the widespread concern in shipbuilding engineering. However, the range of model fidelity still remains considerable uncertainty when simulating the interaction of waves with offshore structures when using numerical methods. To deeply understand these issues, the wave-structure interaction and the wave evolution of the focused waves are studied in this paper.

It is known that the focused wave has significant characteristics of randomness. Thus the real sea state statistics can be hardly recorded. One striking case is the "New Year Wave" which happened in the central North Sea at Statoil Draupner Platform on Jan 1st, 1995. The peak crest elevation reached 18.5m, while the significant wave height

there is 12m. (Bihs et al., 2017) Currently, as the rare appearance of focused waves in nature, the main approaches to study its generation and hydrodynamic properties are experimental and numerical methods.

Experiments are usually carried out in water flumes using wave paddles to generate focused waves. By adopting a focused wave group, many irregular wave components in a spectrum will focus at the designated time and place simultaneously. Previous method included frequency focusing method (Chaplin, 1996) and modified phase and amplitude wave maker control signal to make optimized focused waves (Schmittner et al., 2009). Nevertheless, the effectiveness of their linear wave theory decreases when solving wave groups with high non-linearity. Buldakov, Simons and Stagonas (2014) implement an empirical iterative methodology which can generate focused waves at designated time and space with any height. By controlling the frequency spectrum and phase of the wave components, the extreme wave profile can be formed in a short time and focused at the designated time and location, this make the physical experiments and numerical simulation more efficient. Several experiments are done to investigate the focus waves and the interaction between wave and structure. Liu, Zang and Ning (2009) conducted experimental and numerical studies about a series of steep focused wave groups in a water flume. By using high order boundary element method, their calculation results fitted the experimental results well, even for the waves near to breaking. As for high-order boundary element method, a domain decomposition technique is implemented by Bai and Taylor (2007) to make this method more efficient. To investigate the wave-structure interaction, a simplified FPSO model was set in the Ocean Basin at Plymouth University's COAST Laboratory (Mai, et al., 2016). This experiment took the model length, focused wave steepness and incident wave angles into account. Results were given and analyzed with a general phase-based harmonic separation method. Besides, based on the experiment of COAST laboratory, several numerical methods are used for further researches. Based on the fully nonlinear potential theory (FNPT), Greaves, Ma and Yan (2015) used the Quasi Arbitrary Lagrangian Eulerian Finite Element Method (QALE-FEM) combined with modified time domain self-correction technique. The results are in

good agreement with the experimental results. Greaves, Hu, Mai and Raby (2016) then took the advantage of the computational fluid dynamics to do corresponding numerical simulations using open source code OpenFOAM. The comparison of calculation results shows OpenFOAM is reliable to solve the hydrodynamic problems of wave-structure interaction.

In present studies, computational fluid dynamics (CFD) method based on Navier-Stokes equations is used to solve high non-linear free surface focused wave problems and wave-structure interaction problems. With high performance computers, this numerical method is more popular in shipbuilding and ocean engineering field. Considering the fluid viscosity, the results of CFD method are closer to physical experimental results. Currently, this method is gradually recognized by engineering designers. Plenty numerical simulations and validation works have been done by researchers throughout the world. This calculation method can be divided into Euler method and Lagrange method. The former method use meshes to calculate the velocity, pressure and other parameters in the global flow field. The free surface capture methods include VOF and Level set methods. Through calculating the water and air fraction in each mesh, VOF is able to show the free surface information. Focusing on the problems of extreme waves, Greaves, Westphalen and Williams (2012) adopted commercial CFD packages STAR-CCM+ and Ansys CFX 11 using a finite volume approach and a control-volume finite element method to do numerical calculations. The advantages of CFD method comparing to the potential and experimental method were explained. The results showed that CFD tools are powerful for offshore structure design, and able to solve high non-linear interaction problems. Chen, Hillis and Zang (2014) applied open source code OpenFOAM to assess its performance when solving the non-linear wave-structure interactions. The results showed OpenFOAM could model this problem accurately, capture up to fourth order harmonic and depict the whole field information. Another OpenFOAM application case was made by Greaves, Hu and Raby (2016). The focused waves were generated using new wave boundary condition. The work in this article was systematic and logical. Again, the reliability and accuracy of OpenFOAM was proved. Level set is another method to depict fluid free surface. The open source CFD code REEF3D is commonly used to solve various wave hydrodynamics and wave-structure interaction problems in ocean and offshore engineering based on level set method. Bihs, Chella and Kamath (2016) conducted and evaluated a series of numerical simulations about plunging breaking wave forces which impacted on the vertical cylinder using REEF3D. In the simulation, the breaking process could be showed visually and clearly. Bihs, Chella and Kamath (2017) simulated the interaction between focused waves and vertical cylinder, together with the analyze of the breaking focused waves using REEF3D. Besides, a flexible Lagrangian technique of CFD, smooth particle hydrodynamics (SPH), has been used to simulate various wave-structure interaction problems. Non-linear wave profiles and dynamics are studied using SPH method by researchers (Omidvar, 2010; Lind et al., 2016). With regard to the discretization scheme, finite element method (FEM) has been also adopted in some studies, Hildebrandt and Sriram (2014) used FNPT-FEM to simulate the focused wave interaction with a cylinder. The numerical results were verified and the features of pressures on the cylinder surface and the vortex shedding around the cylinder were discussed. It shows that SPH method is also a reliable method for wave-structure interaction problems. In addition to above method, a fully nonlinear potential flow solver combined with CFD solver was adopted by Bingham, Bredmose and Paulsen (2014) to make the calculation more efficient. Four different complex cases were conducted. The good comparison with experimental results showed that this method is feasible.

The objective of this paper is to do numerical simulations of focused waves with three wave steepness, and then calculate the pressure on the surface of a simplified FPSO model. The open source toolbox OpenFOAM is used in this paper, employed with our in-house 3D viscous flow solver (naoe-FOAM-SJTU) to generate requested focused waves. Firstly, the time histories of focused waves at the specific wave gauges are calculated and verified with CCP-WSI experimental results. After that, the focused wave interaction with FPSO model is simulated. The surface elevation near the FPSO hull is showed, and the pressure data corresponding to three cases are given. The non-linearity of the wave-wave interaction, wave elevation phenomenon and wave load on the structure characteristic are discussed.

## NUMERICAL MODEL

The numerical simulation of two phase flow in this paper adopt our in-house solver naoe-FOAM-SJTU (Shen et al., 2014) which is based on the default solver interDyFoam in OpenFOAM. For wave-structure interaction problems of ocean engineering and hydrodynamics of ship motion, modules of wave generation/damping and six-degree-of-freedom (6DOF) and others are developed and integrated into this solve. For Reynolds number is relatively small in wave generation simulation, the laminar model is selected, which means the turbulence model is not considered when solving the Navier-Stokes equations. The relevant mathematical formulas details used in this solver can be seen as following.

### Governing equations

The fluid here is considered as unsteady, incompressible with viscosity. Firstly, the Navier-Stokes equations are integrated and calculated over the whole space and time domain. The N-S governing equations are:

$$\nabla \cdot U = 0 \quad (1)$$

$$\frac{\partial \rho U}{\partial t} + \nabla(\rho(U - U_g)U) = -\nabla P_d - g \cdot x \nabla \rho + \nabla(\mu \nabla U) + f_\sigma \quad (2)$$

Where  $\rho$  is the density of the water, which is  $1000kg/m^3$  in this paper;  $g$  and  $\mu$  denote the gravity acceleration vector and the dynamic viscosity of fluid respectively;  $U$  is the velocity of the fluid while  $U_g$  is the velocity of grid nodes;  $P_d = P - \rho g \cdot x$  is dynamic pressure of the fluid flow field.  $f_\sigma$  here represents the source item. The solution is discretized into cells and time steps. The pressure-velocity coupling is solved by PIMPLE algorithm with an iterative procedure.

### Free surface capture

In present work, the volume of fluid (VOF) method is applied to capture the interface by tracking the water and air fraction in each cell (Hirt and Nichols, 1981). If the volume fraction value is  $\alpha$ , the state of each cell is as following:

$$\alpha(x, t) = \begin{cases} \alpha < 1 & \text{water} \\ 0 < \alpha < 1 & \text{air} \\ \alpha = 0 & \text{free surface} \end{cases} \quad (3)$$

Usually, the contour with the cell volume fraction  $\alpha = 0.5$  is extracted to represent the free surface. The advantages, such as good mass conservation, computational efficiency, and easy implementation, make VOF method become one of the most popular methods. (Cao, et al.,

2015)

### Discretization Schemes

Over the calculation, the RANS equations and the VOF transport equation are discretized by finite volume method (FVM). Implicit Euler scheme is selected for the temporal discretization. For the convection terms of RANS equations and the diffusion term, the second-order TVD limited linear scheme and the second-order central difference scheme is applied respectively.

### Wave generation and Sponge layer

Before the calculation of the pressure on the structure, the part of wave generation is of vital importance, since it will affect the accuracy of the results. Different from the wave paddle used in physical experiments, the wave is generated directly by inputting the incident wave profile and velocities of water particles at the inlet boundary. The focused wave is generated based on the irregular wave generation method, which is under the assumption that the crest of each wave component coincides at the expected time and position. Introducing the NewWave concept, the average shape of large crest extreme wave can be generated without long-term random wave time series. (Zang et al. 2006) Here the amplitude of the free surface is regarded as linear superposition of regular wave components. The first-order interface can be described as:

$$\eta(x,t) = \sum_{j=1}^N A_j \cos(k_j x - \omega_j t - \varepsilon_j) \quad (4)$$

Where  $\eta$  is the elevation of the free surface,  $N$  is the total number of the wave components.  $A_j$  is the amplitude of the wave component  $j$ , whose angular frequency, wave number and phase is  $\omega_j$ ,  $k_j$  and  $\varepsilon_j$  respectively. To ensure the amplitude of each wave component focus at a specified time  $T_f$  and location  $X_f$ . Phase  $\varepsilon_j$  will be set as follow equation:

$$\varepsilon_j = k_j X_f - \omega_j T_f \quad (5)$$

In terms of wave spectrum  $S_j(\omega)$  and the amplitude  $A_f$  at the focused position, the amplitude  $A_j$  of each component can be expressed as:

$$A_j = A_f \frac{S_j(\omega) \Delta \omega}{\sum_{j=1}^N S_j(\omega) \Delta \omega} \quad (6)$$

The JONSWAP spectrum is used to generate irregular wave components in this paper. The significant wave height  $H_s$ , peak angular frequency  $\omega_p$  and component number  $N$  are inputted to the JONSWAP spectrum.

$$S_j(\omega) = \frac{5}{16} H_s^2 \omega_p^4 \omega_j^{-5} \left(-\frac{5}{4}\right) \exp\left(\left(\frac{\omega_j}{\omega_p}\right)^{-4}\right) \gamma^{\exp\left(\frac{-(\omega-\omega_p)^2}{2\sigma^2 \omega_p^2}\right)} A_\gamma \quad (7)$$

Same with the physical wave tank, waves are also absorbed at the end of the tank in numerical wave tank to reduce the wave reflection from outlet boundary. The wave absorbing method is added in naoe-FOAM-SJTU solver. Sponge layer is applied by adding an artificial viscous

term to the source term of the momentum equation. The term is expressed as:

$$f_s = -\rho \mu_s U \quad (8)$$

Where  $\mu_s$  is the artificial viscosity set by the following equation:

$$\mu_s(x) = \begin{cases} \alpha_s \left(\frac{x-x_0}{L_s}\right)^2, & x > x_0 \\ 0, & x \leq x_0 \end{cases} \quad (9)$$

Where  $\alpha_s$  is damping strength coefficient for the sponge layer.  $L_s$  is the length of the sponge layer, and  $x_0$  is its beginning position. It can be understood more clearly to see the Fig.1 below.

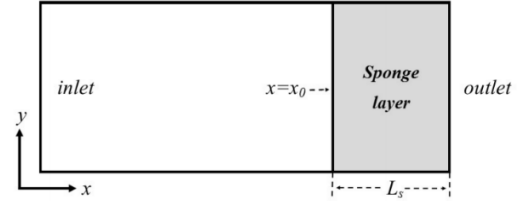


Fig. 1. A diagram of the position of sponge layer in computational domain

### CASE DESCRIPTION AND NUMERICAL DOMAIN

In this paper, a fixed FPSO simplified model is subjected to three focused waves with different wave steepness ( $kA=0.13, 0.18$  and  $0.21$ ) and the same incident angle  $0^\circ$ . Forces are calculated and compared to assess the influence caused by the factor of wave steepness.

### Physical model and experimental configuration

The physical experiment is conducted at COAST laboratory Ocean Basin in Plymouth University. Fig.2 shows the main dimension of FPSO model and wave gauge positions set in wave tank.

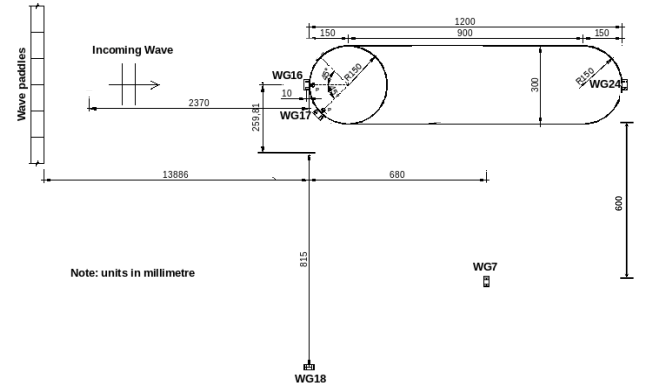


Fig. 2. The wave gauge 16, 18, 17, 24 and 7 layout (with or without FPSO)

The pressure sensor layout on the bow of FPSO in physical experiment is shown as Fig.3.

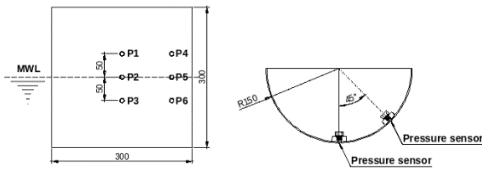


Fig. 3. Pressure sensor P1-P6 layout on the bow of the FPSO model

### Calculation domain and mesh details

According to the requirements of physical experiment, a rectangular shaped computational domain is built as the model of numerical wave tank (NWT). The sketch of computational domain is demonstrated as Fig.4. The length, width and the depth of the NWT is 23m, 4m and 2.93m respectively. The FPSO model is set at the waves focused position, the distance from the bow and the inlet boundary is 13.886m. For preventing the reflection of the waves at the end of the numerical wave tank, a 3-meter length sponge zone is set near the outlet boundary to reduce wave amplitude.

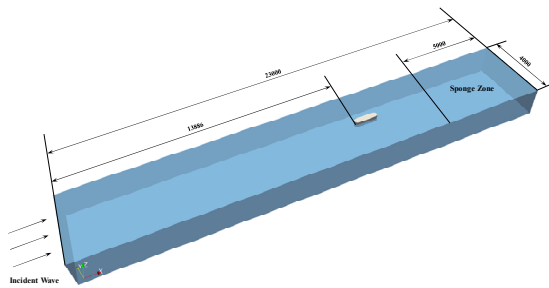


Fig. 4. The numerical wave tank computational domain (with or without FPSO)

The meshes are generated by the tools in OpenFOAM, and the mesh detail is shown as Fig.5.

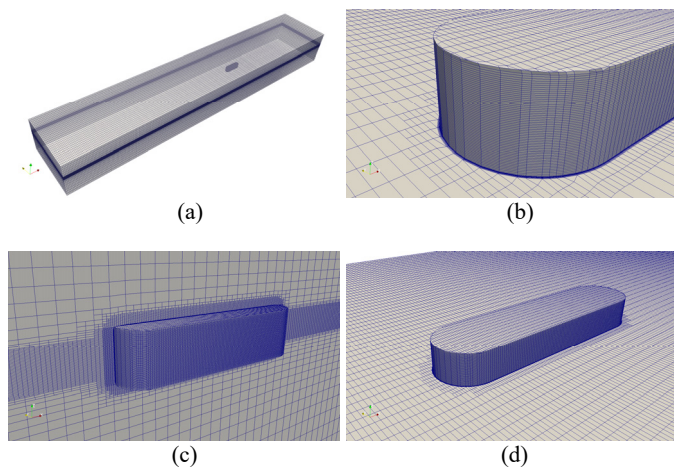


Fig. 5. Mesh detail for calculation: (a) global mesh; (b) bow; (c) longitudinal section; (d) transverse section

Firstly, the background mesh is drawn using blockMesh utility, after that the tool snappyHexMesh is adopted to refine the free-surface layer and the area near the FPSO hull. To ensure the steady propagation and

lower damping of focusing waves, in free-surface mesh refinement layer, the number of the grid is more than 40 in one focused wave height and more than 80 in one characteristic wavelength. Usually, as the reflection effect of the structure, the wave flow field is more complex around the FPSO hull, hence the mesh near the FPSO is also refined.

### Convergence verification

It is well known that mesh quality is of vital importance in CFD numerical simulations. A well designed mesh can improve both the accuracy and efficiency of the simulation. Here, mesh convergence verification is carried out by comparing the results of three mesh densities. Focused waves are generated in test cases. The significant wave height selected here is  $H_s = 0.103m$  and the peak period is  $T_p = 1.456s$ . As described in experiment configurations, wave group contains 244 components with frequency evenly separated between 0.01563Hz and 2 Hz. The focused location is  $x_f = 13.886m$  from inlet boundary. The mesh quality is divided into three level, which are coarse, intermediate and fine meshes. The cell numbers of each level are 76w, 249w and 691 respectively. Because the proper time step has not been found, a temporary selection of time step here is 0.01s. And the amplitude of the focused wave used here is 0.08m.

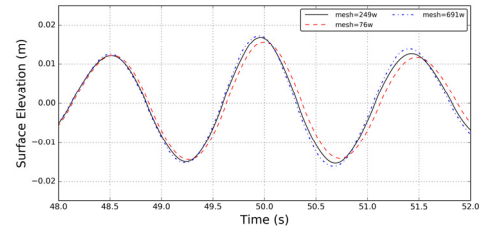


Fig. 6. Wave elevation at the focused position using different meshes

Considering the accuracy and efficiency of the calculation, intermediate mesh is selected, and its detail is shown in Fig.5. While one thing should be noticed that from the Fig.6 the focused wave amplitude is far lower than the expected height no matter how fine the mesh is. This is because the time step 0.01s selected here is too large, wave damping happens during the wave propagation process. So the time step convergence verification is conducted afterwards. Several time steps are selected, including  $\Delta t=0.001s$ ,  $0.0005s$  and  $0.0003s$ . With the time step decrease, the simulation time become longer. The corresponding results can be seen at Fig.7.

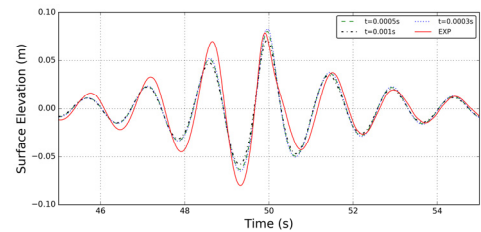


Fig. 7. Wave elevation at the focused position using different time steps

The amplitude parameter of the focused wave used in these time step convergence verification cases is 0.09128m, the same as the physical experiment configuration. Through the comparison between CFD results and experimental results, it can be known that the time step of  $\Delta t = 0.0005m$  is the most suitable value to adopted in following work among three cases. Comparing with the experimental results, the wave

crest at the focused position agree better than the wave trough. The wave profile after the focused time match the target results very well both in wave height and period, while the wave amplitude before the focused time is lower than experimental results. One of the possible reasons is the difference of wave generation methods between numerical simulation in this paper and the physical experiment. This result in the focused wave profile cannot match the experimental results perfectly.

### Computational cases

The numerical verification cases are set following the configuration of the experiments carried out in COAST laboratory. The parameters in three cases with increasing wave steepness are shown as Table 1.

Table 1. Wave parameters for each of the test cases

CCP-WSI ID	$A$ (m)	$T_p$ (s)	$H$ (m)	$H_s$ (m)	$kA$	Alpha (rad)	Phi (rad)
11BT1	0.06914	1.456	2.93	0.077	0.13	0	$\pi$
12BT1	0.09128	1.456	2.93	0.103	0.18	0	$\pi$
13BT1	0.09363	1.362	2.93	0.103	0.21	0	$\pi$

## RESULTS AND DISCUSSIONS

In this section, simulations of focused waves with different incident steepness in empty NWT module are presented and verified with experimental results. After that, the FPSO benchmark model is set into the computational domain. Numerical simulations of wave interaction with FPSO hull are given. The global and local evolution of the free surface are also presented and analyzed.

### Wave elevation validation of focused waves in empty NWT

To validate our in-house hydrodynamics solver, cases with the same parameters of the experiment are simulated. Numerical wave elevation results are demonstrated as Figs. 8~10.

#### Case1 11BT1-Wave elevation comparison ( $kA=0.13$ )

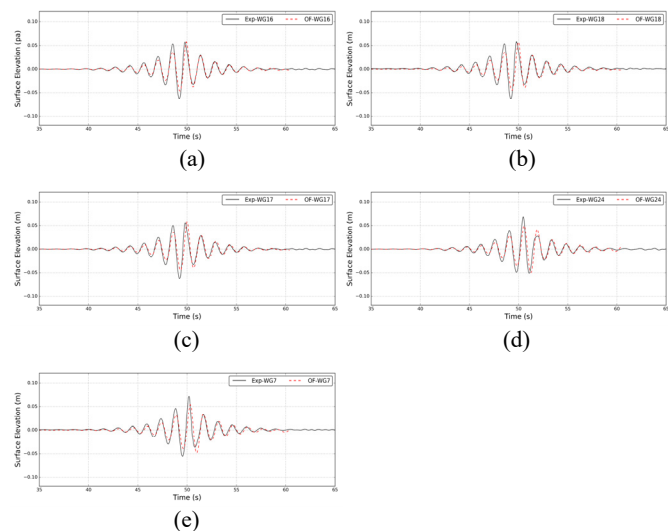


Fig. 8. Time series of the surface elevation at WG 16, 18, 17, 24 and 7 (a-e)

#### Case2 12BT1-Wave elevation comparison ( $kA=0.18$ )

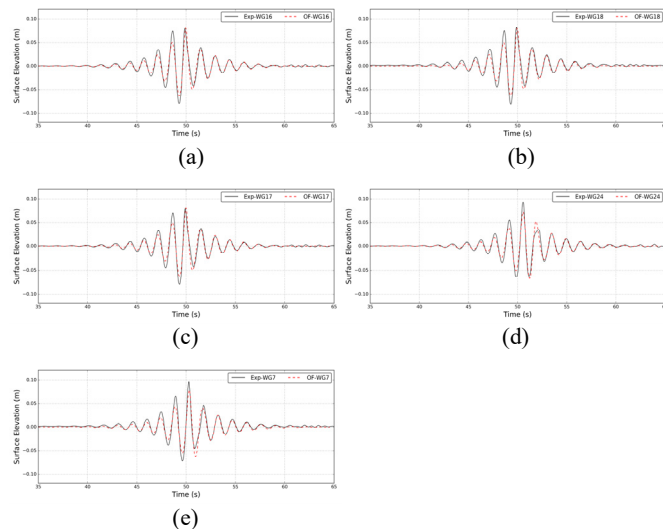


Fig. 9. Time series of the surface elevation at WG 16, 18, 17, 24 and 7 (a-e)

#### Case3 13BT1-Wave elevation comparison ( $kA=0.21$ )

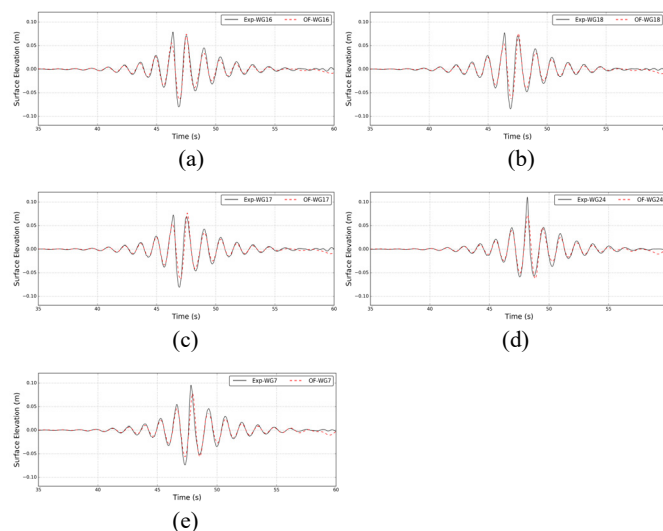


Fig. 10. Time series of the surface elevation at WG 16, 18, 17, 24 and 7 (a-e)

Before calculating the wave pressure on the fixed FPSO hull, the wave generation in empty numerical tank must be carried out and verified with experimental results. From Figs. 8~10, it can be observed that the wave elevation time-history line agree well with the experimental results in general, and they are in better agreement with each other at the time after focused time. However, with the increasing of the wave steepness, non-linear phenomenon is more apparently. Wave-wave interaction happens during the wave propagation process, which will shift the focused time and position deviating from the theoretical value. For example, the focused time in 11BT1 and 12BT1 cases are set at 50s, but there are small offsets in these two cases. Waves recorded at WG16 focused ahead of the theoretical focused time.

Comparing the wave elevation at bow and stern of FPSO between numerical and experimental results (see WG16 and WG24 in Figs. 8–10), it can be seen that the wave elevation results at WG16 of two methods agree well. It shows that the generated waves meet the requirements of next simulations to calculate the pressure on the bow of FPSO model. As for results of WG24, it can be found that experimental results are slightly larger than numerical results. This maybe because the wave damping in numerical simulations and the different actual focused positions. We also notice that the experimental wave elevation results of WG24 are larger than that of WG16. This phenomenon may illustrates that the wave actually focus at the place after theoretical focused position.

From overall results and comparison work, our hydrodynamics solver can be proved to be reliable. The wave generated above can be used to simulate the interaction between focused waves and FPSO-like structure.

### Wave interaction cases between focused waves and FPSO model

The fixed simplified FPSO model in NWT is set at the same position of physical wave tank, where the bow of FPSO is 13.886m away from the front boundary of wave tank. Result from the reflection on the bow of FPSO hull, the wave profile will be deformed. The flow field around the FPSO hull near the theoretical focused time is shown as Fig. 11. It can be observed that the wave run-up and the interface decline phenomenon happen when the incident wave encounter and pass the FPSO hull. Blocked by the FPSO hull, waves will pass through sides and underneath the hull. As the U magnitude distribution on the field longitudinal section shows, the wave diffraction will generate a fast flow (i.e. vortex) at the corner of the hull. Thus a large amount of wave energy is consumed during the wave propagation process. Hence the interface elevation at the stern will be lower than that without FPSO.

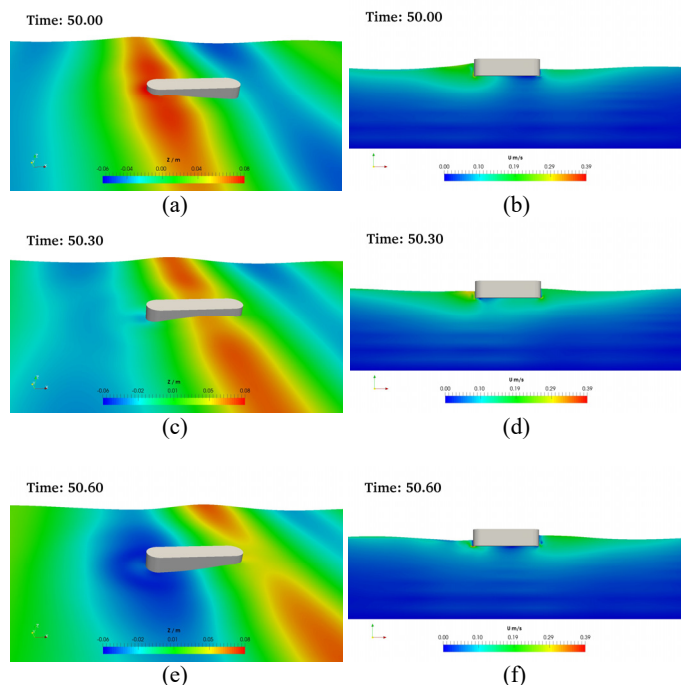


Fig. 11. Instantaneous free surface (a, c and e) and U magnitude (b, d and f) of local field when focused wave passing FPSO (Case 12BT1)

From Fig. 12, the results of wave surface elevation at FPSO bow (WG16) and FPSO stern (WG24) are compared with the corresponding results in NWT without FPSO. It can be found that the diffraction enhanced the surface elevation near FPSO bow, about 12.2%, 27.4% and 26.4% in 11BT1, 12BT1 and 13BT1 cases respectively. It can also be seen that the surface elevation is suppressed after putting the FPSO into the wave tank. The declined surface elevation is approximately 27.6%, 21.3% and 21.1% in 11BT1, 12BT1 and 13BT1 cases.

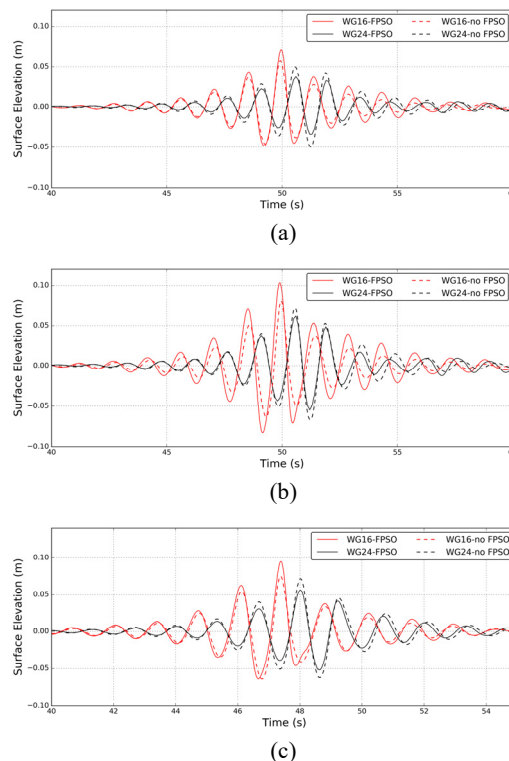


Fig. 12. Comparison of the surface elevation at bow and stern in cases with and without FPSO (a) 11BT1; (b) 12BT1; (c) 13BT1

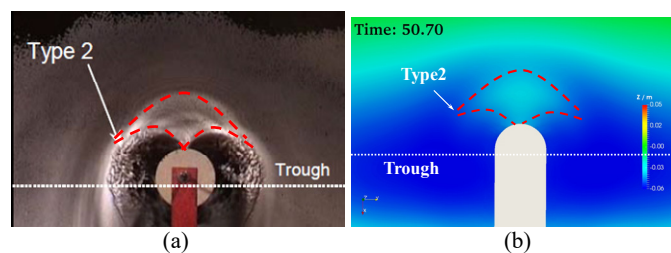


Fig. 13. Instantaneous free surface comparison between experiment and numerical simulation. (a) Experiment photo (b) Simulation screenshot

Meanwhile, during the simulation process, local instantaneous free surface elevation details can be captured and displayed. The wave profile around the structure can be compared with experimental phenomenon. Fig.13 (a) shows a wave type observed in experiment about the interaction between focused wave and vertical cylinder. (Swan et al., 2003) By comparing the experimental and numerical result which is shown as Fig.13 (b), it can be observed that the simulated wave profile is quite similar with actual physical phenomenon when the wave trough encounters the structure. This is because the FPSO model used here can be regarded as a lengthened

cylinder along the x-axis. This comparison shows that OpenFOAM can display the flow field information quite well.

Comparison of physical and numerical measured pressure at the specific position on the bow of FPSO is shown as Figs. 14–16. The pressure sensor layout can be seen as Fig. 3. Among these sensors, P1-P4, P2-P5 and P3-P6 are in the same height but different x coordinates. So their results are combined into each figure separately.

#### Case4 11BT1 – Calculated Pressure on FPSO Bow

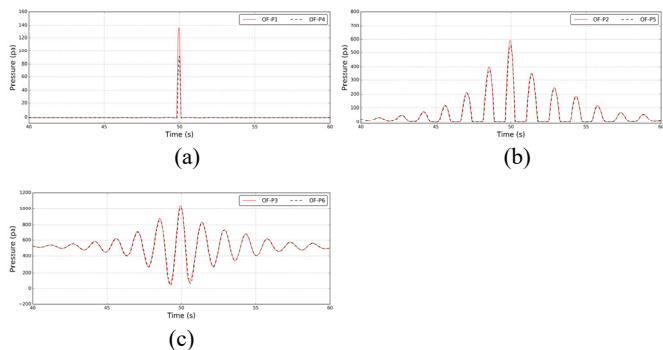


Fig. 14. Calculated pressure of P1-P4, P2-P5 and P3-P6 (a-c) on the bow of the FPSO

#### Case5 12BT1 – Calculated Pressure on FPSO Bow

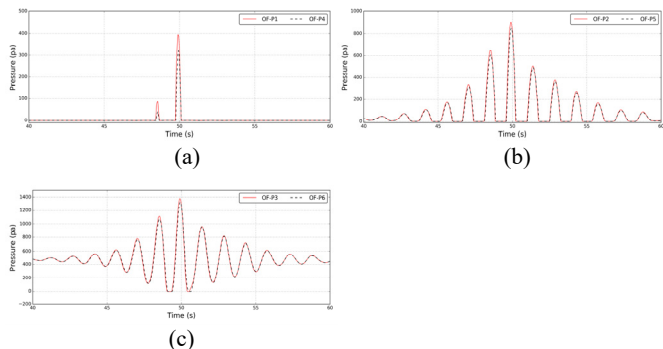


Fig. 15. Calculated pressure of P1-P4, P2-P5 and P3-P6 (a-c) on the bow of the FPSO

#### Case6 13BT1 – Calculated Pressure on FPSO Bow

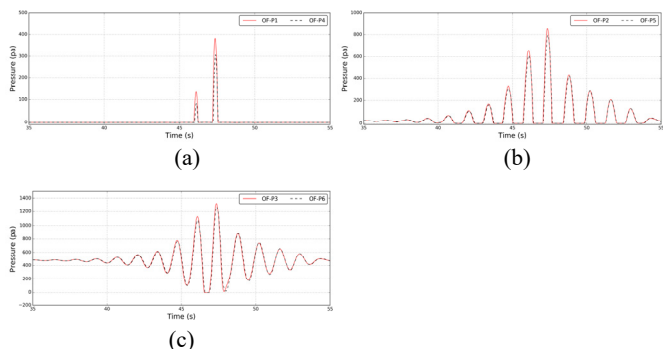


Fig. 16. Calculated pressure of P1-P4, P2-P5 and P3-P6 (a-c) on the bow of the FPSO

The general comparison shows that the pressure measured at P1-P3 are higher than that at P4-P6, especially between P1 and P4 in each case. These three cases have studied the influence of different focused wave characters on wave pressures from two aspects. First one is to compare the effect made by two kinds of focused waves with the same characteristic period and different wave heights. (see Fig.14 and Fig.15) The second aspect is to compare the effect made by focused waves with the same significant wave height and different characteristic periods. (see Fig.15 and Fig.16)

Comparison of pressure results of 11BT1 and 12BT1 cases shows that larger wave height and steepness will increase the pressure on the bow of FPSO, especially at 0.05m above the initial free surface. From these results, we also find that this influence will decline with the increase of the water depth, and the difference between the two pressure results in each figure will be smaller, too.

Comparison between the results of 12BT1 and 13BT1 cases shows that the measured pressure of focused waves are close to each other, though the wave steepness is different. Comparing with the case 11BT1, the similar results maybe because the wave height at the focused position is almost the same and the small difference of wave steepness is less significant comparing to the wave height factor. The higher pressure measured in case 5 is probably because of the higher wave elevation at the bow than case6. A slightly difference of the pressure curves is the higher pressure of the first crest in case6 (a) than that in case5 (a).

## CONCLUSIONS

In this paper, the interaction between focused waves and FPSO-like structure are studied. The numerical simulation is conducted by our in-house solver naoe-FOAM-SJTU which is based on the open source code OpenFOAM. The validation work of this solver is done by comparing the numerical wave elevation results with experimental results which carried out by COAST laboratory. The comparison shows that this numerical method is capable for wave-structure interaction problems.

The pressures on the bow of FPSO hull of three cases are calculated and measured during the following numerical simulations. The basic rules observed from these results are discussed in present work, and the result is going to be validated in CCP-WSI blind test. In addition, more related researches can be investigated in following studies, like the offset phenomenon of the focused time and position and the evolution of the breaking focused waves. Besides, as the theoretic focused time related to the time steps in numerical simulations is too large, each case will run on a HPC cluster for several days. So, the optimization of meshes and numerical scheme can also be studied in future studies.

## ACKNOWLEDGEMENTS

This work is supported by the National Natural Science Foundation of China (51490675, 11432009, 51579145), Chang Jiang Scholars Program (T2014099), Shanghai Excellent Academic Leaders Program (17XD1402300), Program for Professor of Special Appointment (Eastern Scholar) at Shanghai Institutions of Higher Learning (2013022), Innovative Special Project of Numerical Tank of Ministry of Industry and Information Technology of China (2016-23/09) and Lloyd's Register Foundation for doctoral student, to which the authors are most grateful.

## REFERENCES

Bai, W, Taylor, RE (2007) "Numerical simulation of fully nonlinear

- regular and focused wave diffraction around a vertical cylinder using domain decomposition,” *Applied Ocean Research*, 29(1–2):55-71.
- Bihs, H, Chella, MA, Kamath, A, et al. (2016) “Breaking wave interaction with a vertical cylinder and the effect of breaker location,” *Ocean Engineering*, 128:105-115.
- Bihs, H, Chella, MA, Kamath, A and Øivind Asgeir Arntsen (2017). “Numerical Investigation of Focused Waves and their Interaction with a Vertical Cylinder using REEF3D,” *Journal of Offshore Mechanics & Arctic Engineering*, 139(4).
- Bingham, HB, Bredmose, H, Paulsen, BT (2014) “An efficient domain decomposition strategy for wave loads on surface piercing circular cylinders,” *Coastal Engineering*, 86(86):57-76.
- Buldacov, E, Simons, R and Stagonas, D (2014). “Focusing unidirectional wave groups on finite water depth with and without currents,” *Coastal Engineering Proceedings*, 1(34), 31.
- Cao, HJ, Wan DC (2015) “RANS-VOF solver for solitary wave run-up on a circular cylinder,” *China Ocean Engineering*, Volume 29, Issue 2, 183–196.
- Chaplin, JR (1996). “On frequency-focusing unidirectional waves,” *International Journal of Offshore & Polar Engineering*, 6(2), 131-137.
- Chen, LF, Hillis, AJ, Zang, J, et al. (2014) “Numerical investigation of wave–structure interaction using OpenFOAM,” *Ocean Engineering*, 88(5):91-109.
- Department, M, Hennig, J, Kosleck, S, Manoeuvring, S, and Schmittner, C (2009) “A Phase-Amplitude Iteration Scheme for the Optimization of Deterministic Wave Sequences,” *ASME 2009 28th International Conference on Ocean, Offshore and Arctic Engineering*. American Society of Mechanical Engineers, 653-660.
- Eatock-Taylor, R, Liu, SX, Ning, DZ, Taylor, PH, Teng, B and Zang, J (2009) “Free-surface evolution and wave kinematics for nonlinear unidirectional focused wave groups,” *Ocean Engineering*, 36(15–16):1226-1243.
- Gibson, R, Swan, C, Taylor, PH, Taylor, RE, and Zang, J (2006). “Second order wave diffraction around a fixed ship-shaped body in unidirectional steep waves,” *Journal of Offshore Mechanics & Arctic Engineering*, 128(2), 89-99.
- Greaves, D, Hu, ZZ, Mai, T, and Raby, A (2016) “A Numerical and Experimental Study of a Simplified FPSO in Extreme Free Surface Waves,” in *Proceedings of the 26th International Ocean and Polar Engineering Conference*, 26 June - 2 July, Rhodes (Rodos), Greece. 1103-1109.
- Greaves, D, Ma, QW, Yan, S, et al. (2015) “Numerical and experimental studies of Interaction between FPSO and focusing waves,” *The International Ocean and Polar Engineering Conference*. June 21-26, Kona, Big Island, Hawaii, USA. 655-662.
- Greaves, D, Mai, T, Raby, A and Taylor PH (2016) “Physical modelling of wave scattering around fixed FPSO-shaped bodies,” *Applied Ocean Research*, 61:115-129.
- Greaves, D, Hu, ZZ, Raby, A (2016) “Numerical wave tank study of extreme waves and wave-structure interaction using OpenFoam®,” *Ocean Engineering*, 126:329-342.
- Greaves, DM, Westphalen, J, Williams, C. JK, et al. (2012) “Focused waves and wave–structure interaction in a numerical wave tank,” *Ocean Engineering*, 45(5):9-21.
- Hildebrandt, A, Sriram, V (2014) “Pressure distribution and vortex shedding around a cylinder due to a steep wave at the onset of breaking from physical and numerical modeling,” *International Offshore and Polar Engineering Conference*, June 15-20, Busan, Korea. 405-410.
- Hirt, CW, Nichols, BD (1981) “Volume of fluid (VOF) method for the dynamics of free boundaries,” *Journal of Computational Physics*, Volume 39, Issue 1, 201-225.
- Lind, SJ, Rogers, BD, Stansby, PK (2016) “Fixed and moored bodies in steep and breaking waves using SPH with the Froude–Krylov approximation,” *Journal of Ocean Engineering & Marine Energy*, 2(3):331-354.
- Omidvar, P (2010) “Wave loading on bodies in the free surface using smoothed particle hydrodynamics (SPH),” University of Manchester.
- Sheikh R, Swan C (2003) “The interaction between steep waves and a surface-piercing column,” *The 22nd International Conference on Offshore Mechanics & Arctic Engineering*. 373(2033):41251-7.
- Shen, ZR, Wan, DC, Wang, JH and Zhao, WW (2014). “Manual of CFD solver for ship and ocean engineering flows: naoe-FOAM-SJTU”. *Technol Rep Solver Man*, Shanghai Jiao Tong University.